Role of Current Driven Instabilities in the Operation of Plasma Contactors Used with Electrodynamic Tethers

A. Gioulekas* and D. E. Hastings†
Massachusetts Institute of Technology, Cambridge, Massachusetts

The collection of current to an electrodynamic tether in low Earth orbit (LEO) is enhanced by a plasma cloud surrounding the anode (called a plasma contactor). The main mechanism by which this is achieved is the scattering, perpendicular to the lines of the magnetic field, of the electrons which enter the plasma cloud. The scattering may be a result of the interaction between the electrons and unstable electromagnetic waves, one example being lower hybrid waves. The boundaries of instability are found for the lower hybrid waves in a parametric study where for the cases of Ar and NH_3 clouds, the density, the ratio of electron to ion temperature, and the composition of the electron population, are varied. The main conclusion is that the lower hybrid waves will be confined to the outer regions of the cloud. These waves have the right properties to scatter electrons. In the high-density (finite-β) regions of the cloud, the lower hybrid instability will be damped. The ion acoustic and Buneman instabilities are also studied parametrically, and their boundaries are found. These modes have approximately the same threshold of instability (in terms of critical current density) as the lower hybrid waves, but they cannot cause perpendicular scattering since they propagate parallel to the lines of force; they increase the plasma resistivity.

Nomenclature

B_0 = magnetic field
C_{si} = acoustic speed for the ith ion species, $(T_e/M_i)^{1/2}$
k = wavenumber; the subscripts $\perp$ and $\parallel$ refer to directions perpendicular and parallel to B_0, respectively
m_j = jth species mass
n_j = number density
q_j = charge
T_j = temperature in energy units
V_A = Alfven velocity, $eB/\sqrt{4\pi\rho}$
V_{Dj} = drift velocity in the ambient ions rest frame, $(V_{Di2} = 0)$
V_{thj} = thermal speed, $(2T_j/m_j)^{1/2}$
β = ratio of the thermal energy density to the magnetic energy density, $\Sigma_j n_j T_j/B_0^2/8\pi$
λ_{Dj} = Debye length, $V_{thj}/\sqrt{2}\omega_{pj}$
ν = complex wave frequency ($\gamma > 0$ denotes instability), $\omega + i\gamma$
ρ = plasma density
ω_{pj} = plasma frequency, $(4\pi n_j q_j^2/m_j)^{1/2}$
ω_{lh} = lower hybrid frequency, $\sqrt{\Omega_e\Omega_i}$
ω_{ne} = electron-neutral collision frequency
ω_j = Doppler shifted mode frequency, $\omega - k_\parallel V_{Dj}$
Ω_j = cyclotron frequency, $q_j B_0/m_j c$

Introduction

ELECTRODYNAMIC tethers have been proposed as a means of generating power in low Earth orbit (LEO). They consist of a long wire with a metallic sphere (electron collector) at one end, which is deployed from a space vehicle. If an electron current can be collected from the ionosphere, the electromotive force, which is generated across the tether as it moves at an angle with respect to the magnetic field lines, will cause a current to flow in a circuit which consists of the electrodynamic tether collecting electrons at one end and expelling them at the other and the lines of the geomagnetic field (the electrons will cross the lines of force close to the geomagnetic poles where these lines converge). The current flow is shown in Fig. 1.

In this fashion, electric energy is generated at the expense of the kinetic energy of the space vehicle, since the vehicle feels a Lorentz force which opposes its motion. If the sign of the current is reversed (this requires a power supply on board the vehicle, which forces current through the tether in opposition to the *emf* generated by the tether motion), the tether can be used as a thruster.

A crucial parameter for the operation of the electrodynamic tether is the value of current which it collects from the ionosphere. In early concepts of the electrodynamic tethers, the ionospheric electrons were collected by large metallic surfaces that intercepted their orbits. For ampere-level currents, it can be shown that the size of the collection area must be so large that the neutral drag on the system will be significant. This has led to research on the use of plasma contactors as a means of collecting large currents without neutral drag.

A plasma contactor is a plasma source which creates a plasma cloud. The plasma cloud acts as an effective collector since it shields the electric field of the anode. The plasma contactors can produce large amounts of plasma for voltage drops of the order of a few tens of volts. The plasma cloud causes the electrons to cross the magnetic field lines and be

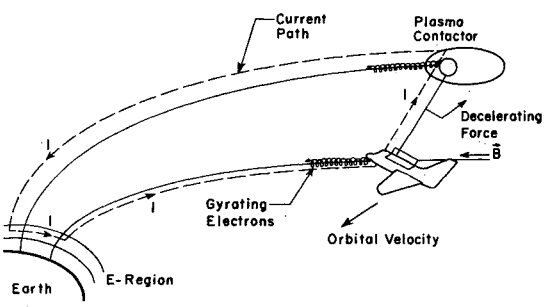

Fig. 1 Electrodynamic tether as a power generator.

Presented as Paper 87-0572 at the AIAA 25th Aerospace Sciences Meeting, Reno, NV, Class of 1956 Career Development, Jan 12-15, 1987. Received May 7, 1988; revision received Dec. 1988.

*Research Assistant.
†Associate Professor, Department of Aeronautics and Astronautics.

diverted towards the anode. There are four possible mechnisms which can cause the ionospheric electrons to move in the above fashion:

a) The plasma cloud can cause the electrons to undergo an $E \times B$ drift across the magnetic field by allowing an azimuthal potential or axial variation of the electric field to develop. This effect can be shown to be small.

b) Classical collisions in the cloud will cause the electrons to undergo a random walk across the magnetic field. This effect becomes significant for densities of the order of 10^{17} particles cm^3. However, for long-term use of plasma contactors, it is necessary to minimize the amount of expelled plasma, and to ensure the desired current. The above value of density is too high for practical purposes.

c) The cloud can shield out the geomagnetic field since plasmas are diamagnetic. This phenomenon occurs in laboratory devices. It will be important in the high-density ($n \geq 10^{10}$ particles/cm^3) regions of the cloud. In this work we discuss the finite-β effects on the operation of the electrodynamic tether system.

d) The cloud can cause electron scattering if it supports microturbulence. The stochastic electric fields associated with the turbulence can cause the electrons to jump across the magnetic field lines. In this work we explore this mechanism. There is experimental evidence that supports the feasibility of electrodynamic tethers as a means of power generation. In ground-based experiments conducted by Patterson,[1] ampere-level electron currents were drawn to plasma contactors over a range of ~ 10 m from a plasma cloud contained in a tank, which was created by ionization of low-density gas by electrons emitted by a hollow cathode. The current to the plasma contactor was found to be at first order a function of the gas pressure (therefore density), contactor geometry, expellant type, and potential difference between anode and cathode.

Plasmas can support many different types of instability since a plasma possesses may degrees of freedom. In this work we choose to concentrate in three well known instabilities and evaluate their effectiveness if excited in a plasma contactor cloud. These are the lower hybrid, the ion acoustic, and the Buneman instabilities. All three instabilities can be excited by field-aligned currents, which we expect in a contactor cloud that is drawing current. In our calculations we take into account finite-β effects.

Lower hybrid waves have been studied extensively in the last few years. In work investigating the stability of these waves, three destabilizing mechanisms have been suggested:

a) A relative particle drift between electrons and ions.[2] The source of free energy has been taken to be the cross-field current due to the particle drift. McBride and Hamasaki[3] have included contributions to the cross-field current from density and temperature gradients. Further work[4] has extended the theory to account for finite-β effects. The conclusion from the finite-β investigations is that the lower hybrid mode is stabilized as β increases. The fastest growing mode shifts to longer wavelengths and makes a transition to the ion-cyclotron mode, which has a growth rate much smaller than the ion-cyclotron frequency. Drake et al.[4] show that the growth rate decreases by four orders of magnitude as β increases from 0 to 2.

b) Non-Maxwellian electron distribution functions.

c) Field-aligned currents: Papadopoulos and Palmadesso[5] have performed an analytic treatment of the instability of electrostatic lower hybrid waves in homogeneous plasmas and found that electron beams could destabilize modes with phase velocities that reside on the positive slope of the electron distribution function.

Migliuolo[6] has derived the linear dispersion relation for a finite-β, in homogeneous plasma with electrons streaming parallel to the magnetic field.

It should be noted that lower hybrid waves are of importance in space plasmas (solar wind and auroral zone).

The neutral stability boundaries for the ion acoustic and Buneman instabilities are solutions of the same dispersion relation.

Papadopoulos[7] has investigated the ion acoustic instability. He has solved the dispersion relation analytically for large values of T_e/T_i. His analysis has been done for a plasma with a single ion species and without distinguishing between two electron populations. The main conclusions of his work that only qualitatively apply to the present problem are the following: a) both the critical drift velocity and the growth rate depend critically on the ratio T_e/T_i, b) $V_{the} > V_{Dcrit} > C_s$, and c) $\omega_{crit} \approx \omega_{pi}$. Hastings[8] has examined the effect of ion acoutic instability on the current flow through a plasma cloud.

The nonlinear theory of the ion acoustic instability has been the subject of controversy. Investigators agree on the fact that stabilization occurs because of effects of the turbulence on the ions. The electron trajectories are not significantly altered by the presence of the acoustic turbulence.[9]

The Buneman instability occurs when there is an electron and an ion distribution function displaced relative to each other by the drift velocity $V_D \geq V_{the}$. In the case that Buneman[10] and Papadopoulos[7] have considered, the electron and ion distribution functions were delta functions. For this case the dispersion relation in the electron reference frame is

$$\frac{\omega_{pi}^2}{(\omega - kV_D)^2} + \frac{\omega_{pe}^2}{\omega^2} = 1 \tag{1}$$

the maximum growth occurs for $kV_D = \omega_{pe}$ and with $\omega = \omega_r + i\gamma$, one finds

$$\omega_r = \omega_{pe}, \gamma = \frac{\sqrt{3}}{2}\left(\frac{m_e}{2m_i}\right)^{1/3}\omega_{pe} \tag{2}$$

The nonlinear theory of the Buneman instability has also drawn attention. Numerical particle simulation methods give the following description of the evolution of the system. The electrons are initially accelerated until their drift velocity exceeds their thermal speed; at this point the Buneman instability comes into play. The fast momentum loss of the electrons keeps the drift velocity constant and heats the electrons to the point where their thermal speed exceeds their drift velocity. This cycle then repeats itself. There is therefore no constant anomalous resistivity, only a time-dependent one, composed of almost square pulses. Biskamp and Chodura[11] describe the main features of the situation as follows: a) The energy supplied to the system accelerates then heats the electrons, b) the system seems to evolve in a self-similar fashion: $V_D \sim t$, $<E^2>/8\pi nT_e \sim$ const. In particular, the electron distribution function remains self-similar. c) $V_D \approx V_{the}$ to a high degree of accuracy.

Note that we can interpret the lower hybrid instability as an oblique ion acoustic instability. There is a major difference between the two instabilities as far as the operation of electrodynamic tether is concerned. When the perpendicular scattering is most efficient (waves with perpendicular wavelength $1/k_\perp \sim \rho_e$), the former propagates perpendicular to the magnetic field lines, and therefore its presence in the plasma cloud is desirable, whereas the latter propagates mainly parallel to the magnetic field enhances the resistivity of the plasma, and its presence in the plasma cloud is undesirable. For $k\rho_e \gg 1$, the ion acoustic instability can cause scattering across the field lines, but it is clear that the most efficient scattering will occur when the wavelength is of the order of the electron gyroradius.

Basic Assumptions

We have based our analysis on the following assumptions.

1) The plasma is considered to be homogeneous. The justification for this assumption is that we are interested in length scales of the order of the electron gyroradius, which we expect to be much smaller than the bulk inhomogeneity length scale.

2) The plasma has finite-β value. For finite-β plasmas, the diamagnetic current can greatly reduce the local value of B. Previous work[8] dealt only with the case of low-β plasmas.

3) We can neglect the presence of neutrals. This assumption holds under the conditions $\gamma \gg \nu_{en}$ and $\Omega_e \gg \nu_{en}$ (i.e., the electrons are magnetized, and the growth rate of the instability is sufficiently fast).

4) The plasma cloud consists of two ionic species (i_1,i_2) and two populations of electrons: electrons that are accelerated by the electric field (runaway electrons) and in the text are called "streaming"(s), and bulk collisional electrons that are weakly affected by the presence of the electric field and are called "static" (e). The ionic species are the ambient ions (O^+) and the contactor ions (Ar^+ or NH_3^+).

The equilibrium distribution function for particles of the jth species is

$$f_{oj} = n_{oj}\left(\frac{m_j}{2\pi T_j}\right)^{3/2} \exp\left[-\frac{V_\perp^2 + (V - V_{Dj})^2}{V_{thj}^2}\right] \tag{3}$$

These two populations for the electrons are found to be the typical composition of the cloud emitted by a plasma source[16] around an electron collector. For the electrons, two populations arise because the electron collector accelerates the higher-energy electrons to form a tail, and the lower-energy electrons are collisionally damped. Typical numbers associated with hollow cathodes as plasma sources are a low-energy population with an energy of 6 V and mean drift velocity of zero and a high-energy population centered around 40 V.[15]

Linear Dispersion Relation

The modes under consideration have frequencies of the order $\omega^2 \sim \Omega_e\Omega_i$ and perpendicular wavelengths smaller than the electron gyroradius, $b_e = (k_\perp V_{the}/\Omega_e)^2 < 1$. On the other hand, the ion gyroradius is much larger than the perpendicular wavelength. As a consequence, the ions can be taken to be unmagnetized (i.e., follow straight orbits), whereas the electrons are magnetized. We work in the ambient ion ($O^+ \equiv i_2$) rest frame: $V_{Di2} = 0$.

The linear dispersion relation is obtained by standard techniques and is[6]

$$D_{11}D_{12} - \frac{\beta_e}{b_e}\frac{\omega^2}{k_\parallel^2 V_{the}^2} D_{12}D_{21} = 0 \tag{4}$$

where

$$D_{11} = k^2\lambda_{De}^2 + \sum_{i=1,2}\frac{n_i T_e}{n_e T_i}\left[1 + \frac{\tilde{\omega}_i}{kV_{thi}} Z\left(\frac{\tilde{\omega}_i}{kV_{thi}}\right)\right] + \sum_{j=e,s}\frac{n_j T_e}{n_e T_j}\left[1 + \frac{\tilde{\omega}_j}{k_\parallel V_{thj}} Z\left(\frac{\tilde{\omega}_j}{k_\parallel V_{thj}}\right) e^{-b_j} I_o(b_j)\right] \tag{5}$$

$$D_{12} = k^2\lambda_{De}^2 + \Sigma_{i=1,2}\frac{n_j T_e}{n_e T_i}\frac{\tilde{\omega}_i}{\omega}\left[1 + \frac{\tilde{\omega}_i}{kV_{thi}} Z\left(\frac{\tilde{\omega}_i}{kV_{thi}}\right)\right] + \sum_{j=e,s}\frac{n_j T_e}{n_e T_j}\left[1 - e^{-b_j} I_o(b_j)\frac{\tilde{\omega}_j}{\omega}\right] \tag{6}$$

$$D_{21} = \sum_{i=1,2}\frac{n_i T_e}{n_e T_i}\frac{k_\parallel V_{Di}}{\omega}\left[1 + \frac{\tilde{\omega}_i}{kV_{thi}} Z\left(\frac{\tilde{\omega}_i}{kV_{thi}}\right)\right] + \sum_{j=e,s}\frac{n_j T_e}{n_e T_j}\frac{k_\parallel V_{Dj}}{\omega}\left[1 + \frac{\tilde{\omega}_j}{k_\parallel V_{thj}} Z\left(\frac{\tilde{\omega}_j}{k_\parallel V_{thj}}\right) \times e^{-b_j} I_0(b_j)\right] + \frac{\tilde{\omega}_j}{\omega} I_0(b_j) e^{-b_j}\left[1 + \frac{\tilde{\omega}_j}{k_\parallel V_{thj}} Z\left(\frac{\tilde{\omega}_j}{k_\parallel V_{thj}}\right)\right] \tag{7}$$

$$D_{22} = 1 + \frac{\beta_e}{b_e}\frac{\omega^2}{k_\parallel^2 V_{the}^2}\sum_{j=e,s}\frac{n_j T_e}{n_e T_j}\frac{k_\parallel V_{Dj}}{\omega}\left[1 - e^{-b_j} I_0(b_j)\frac{\tilde{\omega}_j}{\omega}\right] \tag{8}$$

where

$$k^2 = k_\perp^2 + k_\parallel^2$$

$$b_j = \frac{k_\perp^2 T_j}{m_j \Omega_j^2}$$

I_o is the modified Bessel function and Z is the plasma dispersion function.[12]

This expression only contains coupling to shear Alfven waves and neglects coupling to compressional magnetosonic waves.

Quasineutrality is expressed by the relation

$$n_e + n_s = n_{i1} + n_{i2} \tag{9}$$

The current density is

$$j = |e|(n_e V_{De} + n_s V_{Ds} - n_{i1} V_{Di1}) \tag{10}$$

Parametric Solution of the Dispersion Relation

Lower Hybrid Instability

Equation (4) contains the independent variables

$$n_{i1},\ n_e,\ T_e, T_s, V_{De}, V_{Ds}, m_{i1}, \omega, k_\parallel, k_\perp \tag{11}$$

We have not included in this group the variables m_{i2},n_{i2},T_{i2} because they refer to the ambient O^+ and are fixed. For the LEO environment, the average values of ion density and temperature are taken to be $n_{i2} = 2 \times 10^5\ \text{cm}^{-3}$, $T_{i2} = 0.1\ eV$.

We solve the dispersion relation for ω and V_{De}. Two reasons motivate the solution with two new variables, which are linear combinations of the above, namely $x(1) = \omega/kV_{thi1}$ and $x(2) = (\omega - k_\parallel V_{De})/k_\parallel V_{the}$. The first reason is that the first new variable is related to the ion Landau damping, which tends to stabilize the wave, and the second is related to the inverse electron Landau damping, which drives the instability. The balance of these terms for neutral stability requires that $x(1) > 0$, whereas $x(2) < 0$. The second reason is that the variables must be of the same order to avoid "narrow valley" effects in the numerical solution and as close to 0(1) as possible for better precision. The variables $x(1)$ and $x(2)$ fulfill these requirements.

The law of conservation of energy applied between the center of the cloud and a point on the cloud's edge yields

$$\frac{1}{2} m e V_{Ds}^2 = e\phi \Rightarrow V_{Ds} = -\sqrt{\frac{2e\phi}{m_e}} \tag{12}$$

$$\frac{1}{2} m_{i1} V_{Di1}^2 = e\phi + \frac{1}{2} m_{i1} V_{Bi1}^2 \Rightarrow V_{Di1} = \sqrt{\left(\frac{2e\phi}{m_{i1}} + 2C_{si1}^2\right)} \tag{13}$$

where V_{Bi1} is the Bohm velocity for the i_1 ion species defined as $V_{Bi1} = \sqrt{2C_{si1}} = \sqrt{2}\sqrt{(T_e/m_{i1})}$, and ϕ is the potential drop across the plasma cloud. Recent plasma contactor experiments[16] suggest that the potential drop across the plasma cloud is of the order of a few tens of volts. In reality the potential profile has to be calculated self consistently, but such a treatment is beyond the scope of the present work. For the purpose of this work and for definiteness, we have taken the potential drop to be $\phi = 10$ V. The potential drop is used only to obtain the drift velocity of the streaming electrons for our calculations. Implicit in this statement is the assumption that the potential drop does not in and of itself give rise to any instabilities. However, if the potential drop is localized in double layers either at the contactor boundary or in the elec-

trode sheath, this assumption about the instabilities may not hold.

Next, we set for simplicity $T_e = T_s$ and $T_{i1} = T_{i2} = T_i$. The value of the wave numbers is $k_\parallel$, $k_\perp$ is determined in the following fashion. We are interested in the wave, which, after it has become unstable, grows fastest. The linear dispersion relation has been solved analytically for the *electrostatic* limit with streaming electrons neglected.[13] Seeking a soluton to $D_{11} = 0$, which satisfies $\omega/kV_{thi} \gg 1$ (minimizing the ion Landau damping) and $|(\omega - k_\parallel/V_{De})/k_\parallel V_{the}| \ll 1$ (maximizing the inverse electron Landau damping), we make use of the large and small argument expansions of the plasma dispersion function and find

$$\omega_r^2 = b_e \frac{k}{k_\perp}\Omega_e\left(\Omega_{i1}\frac{n_{i1}}{n_e} + \Omega_{i2}\frac{n_{i2}}{n_e}\right) \tag{14}$$

$$\frac{\gamma}{\omega_r} = -\sqrt{\pi}\left(\frac{\omega_r - k_\parallel V_{De}}{k_\parallel V_{the}}\right)\Gamma_0(b_e)\exp\left[-\left(\frac{\omega_r - k_\parallel V_{De}}{k_\parallel V_{the}}\right)^2\right]$$

$$+\frac{n_{i1}T_e}{n_eT_{i1}}\frac{\omega_r}{kV_{thi1}}\exp\left[-\left(\frac{\omega_r}{kV_{thi1}}\right)^2\right]$$

$$+\frac{n_{i2}T_e}{n_eT_{i2}}\frac{\omega_r}{kV_{thi2}}\exp\left[-\left(\frac{\omega_r}{kV_{thi2}}\right)^2\right) \tag{15}$$

where $\Gamma_0(b_e) = e^{-b_e}I_0(b_e)$.

The parallel and perpendicular wave numbers at maximum growth for the electrostatic case were found to be

$$\frac{\partial\gamma}{\partial k_\parallel} = 0 \Rightarrow \frac{k_\parallel}{k} \approx \sqrt{\frac{m_e}{m_{i1}}\frac{n_{i1}}{n_e} + \frac{m_e}{m_{i2}}\frac{n_{i2}}{n_e}} \tag{16}$$

$$\frac{\partial\gamma}{\partial k_\perp} = 0 \Rightarrow$$

$$[(1 - 2b_e)\Gamma_0(b_e) + 2b_e\Gamma_1(b_e)]e^{-b_e} = \left(\frac{T_e}{T_i}\right)^{3/2}$$

$$\exp\left[-\frac{(T_e/T_i)}{2}\right] \tag{17}$$

We solve the latter equation numerically for b_e, hence, $k_\perp$, and combining the result with the former equation we calculate $k_\parallel$. We use these values for $k_\perp$, $k_\parallel$ in our finite-β calculations since we expect b_e and $k_\parallel/k$ for maximum growth in this case to have values that are close to the corresponding values in the electrostatic case. This can be confirmed a posteriori from the numerical results. In this fashion we have reduced the parameters of the problem to T_e, n_e, n_s or equivalently to T_e/T_i, n_s/n_e, n_e.

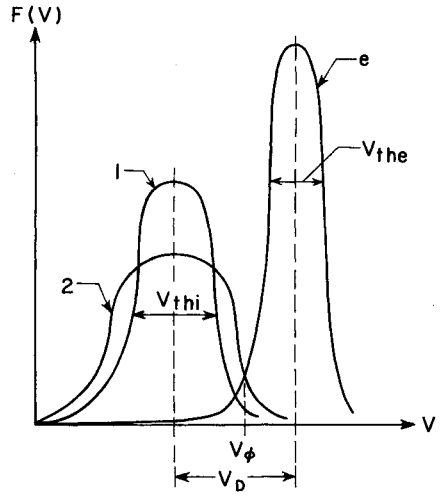

Fig. 2 Typical electron and ion distribution functions as T_e/T_i increases.

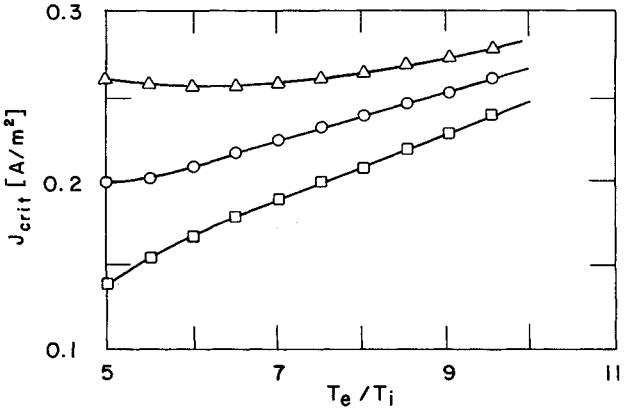

Fig. 3 Lower hybrid instability in a NH_3 cloud, $n_e = 10^6$: critical current density as a function of the ratio of electron temperature to ion temperature; the composition of the electron population varies from $n_s/n_e = 0.1 \rightarrow$ □ to $n_s/n_e = 0.5 \rightarrow$ ○ to $n_s/n_e = 0.9 \rightarrow$ △.

We present our results as follows. For a value of n_e and for three different values of n_s/n_e (usually equal to 0.1, 0.5, 0.9), we plot the critical current density given by Eq. (4) as a function of T_e/T_i, which is taken to vary between the values 5 and 10. This is a reasonable range of values at which the outer edges of the plasma cloud can be expected to operate.

Plots of $x(1)$ and $x(2)$ vs T_e/T_i indicate that the critical drift velocity decreases as T_e/T_i increases. The situation can be explained by referring to Fig. 2. A wave with phase velocity V_ϕ in the region of positive slope of the electron distribution function will be unstable, and will gain energy at the expense of the particle energy. This wave lies on the region of the negative slope of the ion distribution and will be damped by the ions. When the wave is marginally stable, the energy which is added to it by the electrons is subtracted from it by the ions.

As indicated in the figure, $V_{thi1} < V_{thi2} \Rightarrow (T_e/T_i)_1 > (T_e/T_i)_2$. It is obvious that, if in the case of ion distribution function 2, the wave is marginally stable, then in the case of the ion distribution function 1, the wave will be unstable. Hence V_D decreases as T_e/T_i increases.

The natural variable to be used in comparing the effects of different densities, temperature ratios, etc., on the threshold of instability, is the drift velocity of the bulk electrons.

However, we are interested in the application of the numerical results to ascertain the engineering efficacy of contactors used with tethers. For these purposes the absolute magnitude of the current density is the relevant variable.

In Figure 3, we plot the critical current density for triggering the lower hybrid instability of NH_3 where $n_e = 10^6$ cm^{-3}. We see that current density increases with T_e/T_i despite the fact that the critical drift velocity decreases with T_e/T_i. The reason is that the term $n_{i1}V_{Di1} \sim C_{si1} \sim \sqrt{T_e}$ depends more strongly on T_e and is larger than the term n_eV_{De}, and therefore its behavior is the dominant one.

Even though use of the critical current density marks the effect of varying n_s/n_e, we see that increasing the fraction of streaming electrons from 0.1 to 0.9 does not increase the critical current density by a similar factor. This coincides with the physical notion that having more streaming electrons is destabilizing. We note that the $T_e = 0.1$ eV and $n_e = 10^6$ cm^{-3}, the random electron current density is 8×10^{-3} A/m^2, and therefore in order for the parallel electron current to self consistently trigger these instabilities, the random electron current must have undergone some considerable concentra-

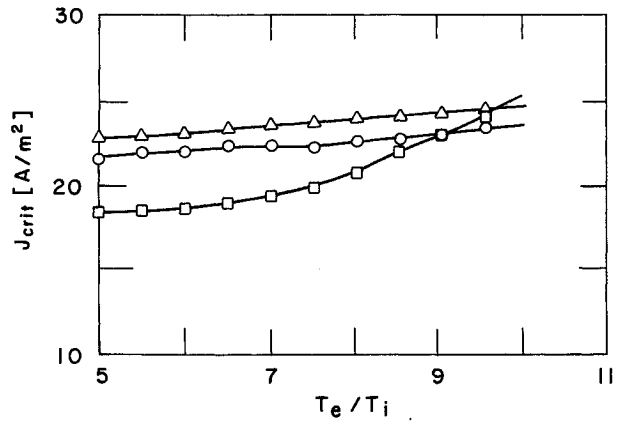

Fig. 4 Lower hybrid instability in a NH_3 cloud, $n_e = 10^8$: critical current density as a function of the ratio of electron temperature to ion temperature; the composition of the electron population varies from $n_s/n_e = 0.1 \rightarrow$ □ to $n_s/n_e = 0.5 \rightarrow$ ○ to $n_s/n_e = 0.9 \rightarrow$ △.

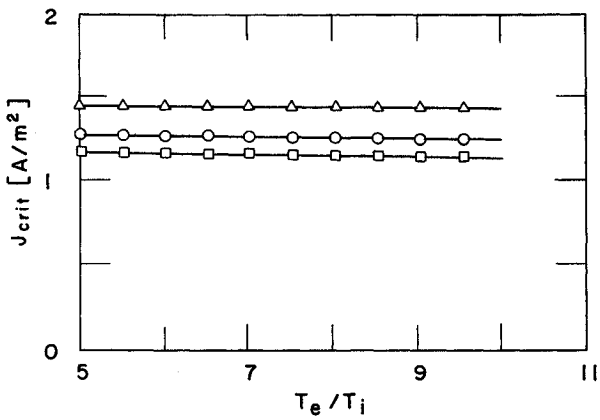

Fig. 5 Lower hybrid instability in a NH_3 cloud, $n_e = 10^{10}$: critical current density as a function of the ratio of electron temperature to ion temperature; the composition of the electron population varies from $n_s/n_e = 0.1 \rightarrow$ □ to $n_s/n_e = 0.5 \rightarrow$ ○ to $n_s/n_e = 0.9 \rightarrow$ △.

tion. This may have occurred in the far outer reaches of the cloud where the electron density is closer to ambient.

In Fig. 4 we consider the lower hybrid instability when the electron density is increased to 10^8 cm^{-3}. This corresponds to a value of $\beta \simeq 10^{-2}$. We see that for $n_s/n_e = 0.1$, the critical current density has increased by more than two orders of magnitude. This clearly indicates the stabilizing effect of the higher plasma density. This is confirmed by increasing the plasma density to 10 cm^{-3} when it is found that there is no instability boundary of $n_s/n_e = 0.1$. This suggests that the lower hybrid instability will be confined to the outer reaches of the plasma cloud if it exists at all.

In Figs. 5 and 6, we consider Argon as the contactor gas for $n_e = 10^6$ cm^{-3} and 10^8 cm^{-3} respectively. Once again we see the stabilizing effect of higher density. For the low-density case we see that for $n_s/n_e = 0.1$, the critical current density decreases as T_e/T_i increases. This corresponds to the electrostatic, no streaming electron result explored[8] where a window of instability was found for large T_e/T_i and where the critical current density was less than the random current density. The reason that the critical current decreases with mass is both due to the decreased ion velocity and also due to the decreased effectiveness of massive ions in Landau damping. Therefore, we conclude that the lower hybrid waves can effectively interact with the streaming electrons.

Buneman and Ion Acoustic Instabilities

These waves are propagating parallel to the magnetic field ($k_\perp = 0$), and the dispersion relation simplifies to the zero magnetic field case.[14]

$$0 = k^2\lambda_{De}^2 + \sum_{i=1,2} \frac{n_i T_e}{n_e T_i}\left[1 + \frac{\tilde{\omega}_i}{kV_{thi}} Z\left(\frac{\tilde{\omega}_i}{kV_{thi}}\right)\right] + \sum_{j=e,s} \frac{n_j T_e}{n_e T_j}\left[1 + \frac{\tilde{\omega}_j}{kV_{thj}} Z\left(\frac{\tilde{\omega}_j}{kV_{thj}}\right)\right] \tag{18}$$

where $\tilde{\omega}_{i,j} = \omega - kV_{Di,j}$.

We note that the above equation can be written as $D_{11} = 0$ with $b_j = 0$, where D_{11} is defined previously.

One may notice that only ratios of the particle number densities enter the dispersion relation, and therefore the solution is expected to be independent of the total electron number density.

The total electron number density comes into play in the following fashion; Kindel and Kennel[14] have found that when $T_e/T_i \gg 1$, the first waves to become unstable have wave numbers: $k\lambda_{De} \approx 1 \Rightarrow k \approx 1/\lambda_{De} \approx \sqrt{(n_e + n_s)/T_e}$. Since we take the wave number in our calculations to be equal to the inverse Debye length, we introduce a dependence on the total electron number density. Therefore, when we multiply the total electron number density by a factor of 10^2, we are in effect seeking the threshold of instability of waves in a plasma with the initial electron number density but with wave number 10 times larger.

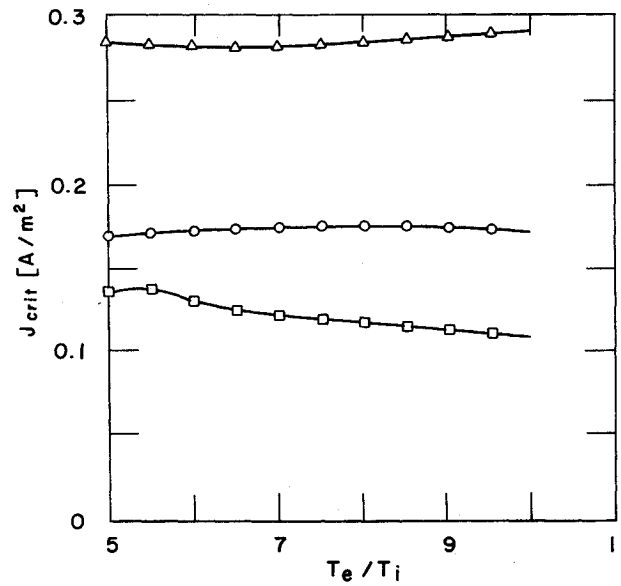

Fig. 6 Lower hybrid instability in a Ar cloud, $n_e = 10^6$: critical current density as a function of the ratio of electron temperature to ion temperature; the composition of the electron population varies from $n_s/n_e = 0.1 \rightarrow$ □ to $n_s/n_e = 0.5 \rightarrow$ ○ to $n_s/n_e = 0.9 \rightarrow$ △.

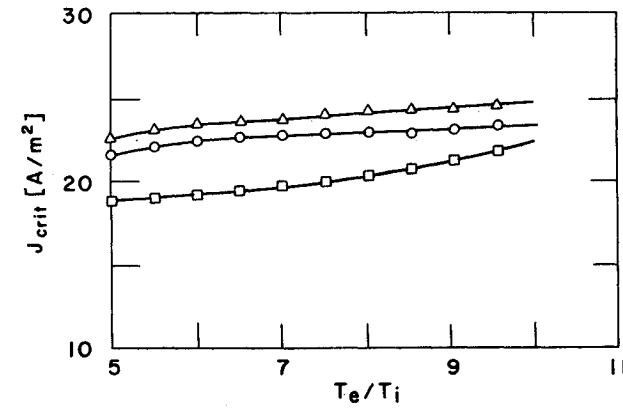

Fig. 7 Lower hybrid instability in a Ar cloud, $n_e = 10^8$: critical current density as a function of the ratio of electron temperature to ion temperature; the composition of the electron population varies from $n_s/n_e = 0.1 \rightarrow$ □ to $n_s/n_e = 0.5 \rightarrow$ ○ to $n_s/n_e = 0.9 \rightarrow$ △.

If $n_{i1} \gg n_{i2}$ then $n_e + n_s \approx n_{i1}$, and the above relation becomes $j_{crit} = |e| n_e(V_{Dcrit} + n_s/n_e V_{Ds} - V_{Di1} - n_s/n_e V_{Di1})$. Therefore, if one divides the value of the critical current density for $n_e = 10^8$ cm^{-3} by 10^2, one obtains the value of the critical current density for $n_e = 10^6$ cm^{-3} for waves with $k = 10/\lambda_{De}$ where λ_{De} is evaluated for $n_s + n_e = 10^6(1 + n_s/n_e)$ cm^{-3}. The rest of the control parameters (note that $k_\perp = 0$) are fixed in the fashion described previously.

In Figs. 7 and 8 we examine the ion acoustic and Buneman instabilities for the outer cloud region where $n_e \approx 10^6$ cm^{-3}. For the ion acoustic instability, we find critical currents of the same order as the lower hybrid instability. Hence, these two will probably coexist in the plasma cloud. This suggests that perpendicular (anomalous diffusion) and parallel (anomalous resistivity) scattering will be inseparable in any contactor cloud. For the Buneman instability, the critical current density is much higher than for the ion acoustic instability as expected from conventional stability theory.

Conclusions – Suggestions on the Form of the Plasma Contactor

Lower Hybrid Instability

We have shown that the lower hybrid instability, which is desirable for scattering electrons across the geomagnetic field inside a plasma contactor cloud, will be confined to the low-density outer reaches of the cloud. This is fundamentally due to the stabilizing effect of the plasma diamagnetism. This suggests that the plasma cloud will have a belt of unstable plasma surrounding a stable core. This belt will serve to concentrate the current density feeding the anodic end of the tether and giving rise to the picture of the contactor as giving a large effective collection area. In order for the concentration to be self consistent for the case of $n_e \approx 10^6$ cm^{-3} the current density will have to be concentrated by a factor of approximately 17. Since current is conserved, we can say that in a self-consistent calculation, the effective collection area of the belt is 17 times the area of the core cloud. For a 1-m radius core region, this would correspond to an effective radius of approximately 4 m.

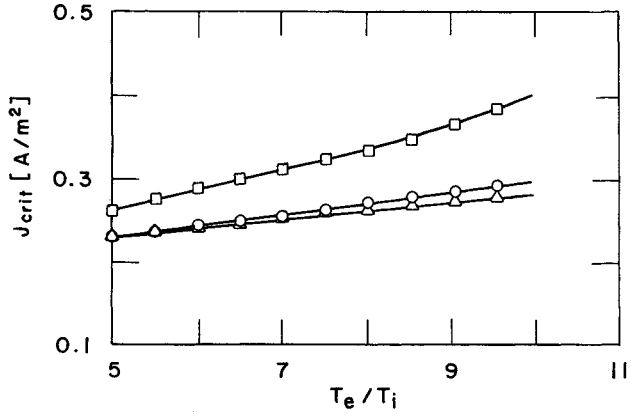

Fig. 8 Buneman instability in a NH_3 cloud, $n_e = 10^6$: critical current density as a function of the ratio of electron temperature to ion temperature; the composition of the electron population varies from $n_s/n_e = 0.5 \rightarrow$ □ to $n_s/n_e = 0.6 \rightarrow$ ○ to $n_s/n_e = 0.9 \rightarrow$ △.

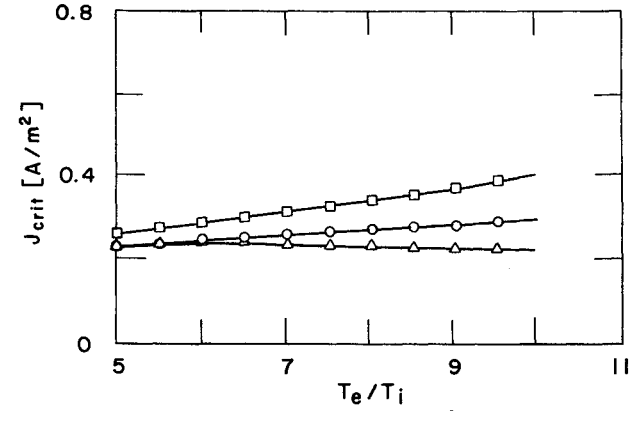

Fig. 9 Buneman instability in a Ar cloud, $n_e = 10^6$: critical current density as a function of the ratio of electron temperature to ion temperature; the composition of the electron population varies from $n_s/n_e = 0.5 \rightarrow$ □ to $n_s/n_e = 0.6 \rightarrow$ ○ to $n_s/n_e = 0.9 \rightarrow$ △.

Table 1 NH_3

n_e (cm^{-3})	10^8	10^{10}	10^{12}
β	$\sim 10^{-4}$	$\sim 10^{-2}$	~ 1
n_s/n_e	0.1 0.5 0.9	0.1 0.5 0.9	0.6 0.7 0.9
J_{crit} (A/m^2)	0.2 0.22 0.27	20 22 23	1200 1300 1400

Table 2 Ar

n_e (cm^{-3})	10^8	10^{10}	10^{12}
β	$\sim 10^{-4}$	$\sim 10^{-2}$	~ 1
n_s/n_e	0.1 0.5 0.9	0.1 0.5 0.9	0.6 0.7 0.9
J_{crit} (A/m^2)	0.12 0.17 0.28	20 22 23	1200 1300 1400

We have also seen that the ion acoustic instability will be excited simultaneously with the lower hybrid instability so that this large effective area will have an anomalous resistivity associated with it.

The difficult question of self consistency will be addressed in a future work.

In Tables 1 and 2, we show how the magnitude of the critical current density varies with β, in the cases of NH_3 and Ar clouds (the value of J_{crit} is averaged over the range $5 < T_e/T_i < 10$).

The current density varies with the distance from the center of the cloud in the following fashion: $J = I/A \sim I/r^2$. Also $\beta \propto n_e + n_s$, where $n_e + n_s$ is the total electron number density.

Suppose that we know the function $J_{crit}(\beta)$. We also know that a region of the cloud at a distance r_1 from the center of the cloud has total electron number density n_1, with a corresponding $\beta_1 = n_1 T_e/B_0^2/8\pi$, and is on the verge of instability. We want to find the condition, which the density n_2 at radius r_2 must satisfy for instability.

From β_1 we find

$$J_1 = J_{crit}(\beta_1);\ J_2 = \frac{r_1^2}{r_2^2} J_1, \beta_2 = \frac{n_2}{n_1}\beta_1$$

therefore

$$J_2 > J_{crit}(\beta_2) \Rightarrow \frac{r_1^2}{r_2^2} J_{crit}(\beta_1) > J_{crit}\left(\frac{n_2}{n_1}\beta_1\right)$$

Our results show that, as the value of β grows, the lower hybrid wave is stabilized (for $n_e = 10^{10}$ cm^{-3} the plasma is stable for values of $n_s/n_e < 0.5$). Previous investigations on finite-β plasmas have reached the same conclusions. This suggests that in the plasma cloud, there will be regions of the cloud ($\beta > 1$, $n_e > 10^{10}$ cm^{-3}) where no instabilities occur, whereas in other regions of the cloud ($\beta \ll 1$, $n_e \ll 10^{10}$ cm^{-3}) the plasma will be turbulent. In the turbulent region, the growing lower hybrid waves will scatter the streaming electrons and cause them to cross the lines of force and be diverted towards the anode. In the infinite-β region of the cloud, however, where there exists no scattering mechanism, the geomagnetic field will be weakened, and the electrons may still be able to cross the magnetic field lines.

If the value of the current density is smaller than the critical current density in the outer regions of the plasma cloud (for

which $\beta \to 0$), the electrodynamic tether will be characterized by high impedance. Since the value of the current density increases as the potential of the anode increases (since more electrons are attracted to the anode), a high impedance mode of operation of the system will switch to a low impedance mode as the value of critical current density is reached in the outer regions of the cloud.

The value of the critical current density for $n_e = 10^8$ cm^{-3} (which corresponds to $n_s + n_e \leq 10^9$ cm^{-3}) is approximately 20 A/m^2, and therefore, since the collection area of the anode will be of the order of 1 m^2, the value of the collected current will be of the order of a few tens of amperes. This value of the collected current is the desired one, when the electrodynamic tether is used as a means of generating power. Thus, for this application, the suggested number density of the core of the plasma is $n_e + n_s \sim 10^9$ cm^{-3}.

It must be determined whether a plasma cloud with this core number density moving at a speed of 8×10^{-3} m/s can retain its coherence. It is suggested that the evolution of the plasma cloud be studied and that a value for the core density be adopted for the engineering application, such that, 1) it be $\geq 10^9$ particles/ cm^3 and 2) the diffusive mechanisms be weak, so as not to destroy the coherence of the plasma cloud.

The dependence of the critical drift velocity on the ratio n_s/n_e varies from case to case, and, therefore, we cannot draw general conclusions on how a change of the ratio n_s/n_e affects the critical drift velocity. In the expression of the critical current density $j_{crit} = |e|\ [n_e(V_{De} + n_s/n_e V_{Ds}) - n_{il} V_{Dil}]$, V_{Ds} has a value such that even a decrease in V_{De} as n_s/n_e increases is compensated by an increase in the term $n_s/n_e V_{Ds}$, so that in general, the value of the critical current density increases as the ratio n_s/n_e increases.

Finally, we note that the values of critical current density for NH_3 are very close to those for Ar. Since NH_3 is lighter than the Ar and can be stored in the liquid state occupying a smaller volume, we suggest the use of NH_3.

Ion Acoustic and Buneman Instabilities

Our results show that as the ratio n_s/n_e increases, the critical drift velocity for the ion acoustic instability increases, whereas the critical drift velocity for the Buneman instability decreases, and for $n_s/n_e = 0.9$, we find that there is only one value of the drift velocity for which instability occurs, i.e., the two instabilities for large values of the ratio n_s/n_e are indistinguishable.

For those values of n_s/n_e, for which we find two distinct solutions of the dispersion relation, the ion acoustic instability is triggered by a smaller current than the Buneman instability. If the current density exceeds both critical values, both instabilities will appear, but since their evolution (as predicted by the nonlinear theory) differs, it will be possible to distinguish them.

For the value of $n_e = 10^8$ cm^{-3} [or equivalently for wave numbers $k = 10/\lambda_{De}$ where λ_{De} is the Debye length for a plasma with $n_s + n_e = 10^6(1 + n_s/n_e)$ cm^{-3}] solutions for neutral stability exist only for values $n_s/n_e \leq 0.1$. Since the small value of the ratio n_s/n_e means that the amount of free energy which can be fed into the waves and cause instability is smaller than the one for larger values of n_s/n_e, we conclude that for values of $n_s/n_e > 0.1$, the waves under consideration are unstable to infinitesimal disturbances, but no conditions for marginal stability exist.

Finally, we note that these instabilities occur for a range of values of the critical current density similar to that for which the lower hybrid instability occurs; thus it is possible that all three instabilities coexist.

Conclusions

In this work we have studied three kinds of the instabilities that are expected to occur in the plasma contactor. The lower hybrid instability has the property to scatter the streaming electrons perpendicular to the geomagnetic field and therefore decreases the impedance of the system. We have computed the stability boundaries of the system, in terms of the current density for marginal stability, with the electron to ion temperature ratio, the ratio of the number of streaming to static electrons, and the relative density of the two electron populations as parameters for various values of the particle number density of the cloud.

We have concluded that as the density increases ($\beta \to 1$), the lower hybrid wave is stabilized. However, in the high density (finite-β) regions of the cloud, the diamagnetism of the plasma becomes important, and the electrons can still cross the weakened magnetic field. It is evident from the above that the impedance of the contactor depends on the collected current; if at a region of the cloud, the value of the current density exceeds the critical value, this cloud region will be turbulent and its impedance will be low. We should caution however that the whole system is highly nonlinear and although we have included the high-β effects on waves and shielding of the geomagnetic field, we have not calculated the self-consistent plasma currents associated with the large plasma β. These may change some of the conclusions about current collection.

The ion acoustic and Buneman instabilities propagate parallel to the magnetic field and therefore do not contribute to perpendicular scattering. Their effect is an increase in plasma resistivity.

The threshold of instability does not differ substantially for the two types of waves considered, and, therefore, only the subsequent behavior of the growing waves will enable us to distinguish one from the other.

We comment that the choice of instabilities to study was motivated by the assumption that the drift velocity of the electrons was at most of the order of the electron thermal velocity. If the drift velocity substantially exceeds the thermal velocity, then the excitation of beam plasma instabilities would be expected. These would require a separate study. A plasma contactor cloud used with an electrodynamic tether, which can generate thousands of volts, can have a large potential drop associated with it. However, if the system is to be competititve as a power system in space, then the potential drop associated with the plasma cloud must be small. We assumed a potential drop of the order of a few tens of volts, which gives drift velocities of the order of the electron thermal velocity. Systems with much larger potential drops through the cloud will have different instabilities since the drift velocity can be so much higher but will not be interesting in an engineering sense.

Acknowledgments

This work was supported by NASA Grant NAG3-681.

References

[1]Patterson, M., "Hollow-Cathode Based Plasma Contactor Experiments for Electrodynamic Tethers," *Proceedings of the 1st International Conference on Tethers in Space*, AIAA, New York, 1986.

[2]Krall, N., and Liewer, P., "Low Frequency Instabilities in Magnetic Pulses," *Physical Review A*, Vol. 4, No. 5, 1971, pp. 2094-2103.

[3]McBride, J., and Hamasaki, S., "Temperature Gradient and Electron Gyroradius Effects on Lower Hybrid-Drift Cyclotron Instabilities," *Physics of Fluids*, Vol. 21, 1978, p. 1979.

[4]Drake J., Hub, J., and Gladd, N., "Stabilization of the Lower Hybrid Drift Instability in a Finite-β Plasma," *Physics of Fluids*, Vol. 26, No. 8, 1983a, pp. 2247-2249.

[5]Papadopoulos, K., and Palmadesso, P., "Excitation of Lower Hybrid Waves in a Plasma by Electron Beams," *Physics of Fluids*, Vol. 19, No. 4, 1976, pp. 605-606.

[6]Migliuolo, S., "Lower Hybrid Waves in Finite-β Plasmas, Destabilized by Electron Beams," *Journal of Geophysical Research*, Vol. 90, No. 41, 1985, pp. 377-385.

[7]Papadopoulos, K., "A Review of Anomalous Resistivity for the Ionosphere," *Reviews of Geophysics and Space Physics*, Vol. 15, 1976, pp. 113-127.

[8]Hastings, D. E., "Enhanced Current Flow Through a Plasma Cloud by Induction of Plasma Turbulence," *Journal of Geophysical*

Research, Vol. 92, No. A7, pp. 7716–7722.

[9]Dupree, T., "A Perturbation Theory for Strong Plasma Turbulence," *Physics of Fluids*, Vol. 16, 1966, p. 1773.

[10]Buneman, O., "Dissipation of Currents in Ionized Media," *Physical Review*, Vol. 115, No. 3, 1959, pp. 503–517.

[11]Biskamp, D., and Chodura, R., "Asymptotic Behaviour of the Two Stream Instability," *Physics of Fluids*, Vol. 16, No. 6, 1973, pp. 888–892.

[12]Fried, B. D., and Conte, S. E., *The Plasma Dispersion Function*, Academic, Orlando, Fla., 1961.

[13]Gioulekas, A., and Hastings, D. E., "Plasma Effects Associated with Contactor Clouds Used in the Ionosphere," AIAA Paper 87-0572, 1986.

[14]Kindel, J., and Kennel, C., "Topside Current Driven Instabilities," *Journal of Geophysical Research*, Vol. 76, No. 13, 1971, pp. 3055–3078.

[15]Wilbur, P., private communication.

[16]Wilbur, P., and Laupa, T., "Plasma Contactor Design for Electrodynamic Tether Applications," *Advances in Space Research*, Vol. 8, No. 1, 1988, pp. 221–224.